

## ORIGINAL ARTICLE

# MiR-200c regulates ROS-induced apoptosis in murine BV-2 cells by targeting FAP-1

DS Yu<sup>1</sup>, G Lv<sup>1</sup>, XF Mei<sup>1</sup>, Y Cao<sup>1</sup>, YF Wang<sup>2</sup>, YS Wang<sup>1</sup> and YL Bi<sup>1</sup>

**Objective:** Reactive oxygen species (ROS) are significantly upregulated after spinal cord injury (SCI). MicroRNAs (miRNAs) are reported to be widely involved in regulating gene expression. This paper aims to explore the correlation between ROS-induced cell apoptosis and abnormal miRNA expression after SCI.

**Methods:** To profile the expression of miRNAs after SCI, miRNA microarray was applied and the result was verified by reverse transcription quantitative PCR (RT-qPCR). ROS production following H<sub>2</sub>O<sub>2</sub> stimulation was examined using dihydroethidium staining and flow cytometry. The levels of miR-200c after H<sub>2</sub>O<sub>2</sub> treatment were determined using RT-qPCR. Cell viability and apoptosis were examined in murine BV-2 cells transfected with miR-200c mimics, inhibitor or negative control. Immunofluorescence and western blot were used to further explore the effects of miR-200c on Fas-associated phosphatase-1 (FAP-1) expression.

**Results:** MiR-200c was showed to be significantly increased after SCI by miRNA microarray and RT-qPCR. ROS production enhanced miR-200c expression in a dose-dependent manner and induced significant apoptosis in BV-2 cells. The upregulation of miR-200c reduced cell viability and induced BV-2 cell apoptosis. MiR-200c negatively regulated the expression of FAP-1, thereby inducing FAS signaling-induced apoptosis. RT-qPCR analysis showed that the FAP-1-targeting small interfering RNA (siRNA) did not affect the level of miR-200c in murine BV-2 cells. In addition, suppression of FAP-1 by siRNA promoted apoptosis, even in cells that were co-transfected with the miR-200c inhibitor.

**Conclusions:** The current data suggested that miR-200c contributes to apoptosis in murine BV-2 cells by regulating the expression of FAP-1. This proposes a therapeutic target for enhancing neural cell functional recovery after SCI.

*Spinal Cord* (2015) 53, 182–189; doi:10.1038/sc.2014.185; published online 2 December 2014

## INTRODUCTION

In spine and neurosurgery departments, spinal cord injury (SCI) is a common devastating injury, which is often caused by accidents and sports injuries. SCI can lead to deadly disabilities, including paralysis and loss of mobility. The main types of cells present in the spinal cord include oligodendrocytes, neurons, astrocytes and microglia.<sup>1</sup> Microglia constitute 5–20% of total glial cells in rodents, depending on the specific neuroanatomical region of the central nervous system (CNS).<sup>2</sup> Microglia cells are different from neuron and other glial cells owing to their origin, morphology, gene expression pattern and function. Microglia-mediated innate immune response in the CNS has key roles in the pathology of a number of CNS neuroinflammatory diseases.<sup>2</sup> To explore the pathologic factors after SCI, the immortalized murine BV-2 cell line was applied as it is reported to share many characteristics with primary microglia.

Reactive oxygen species (ROS), including H<sub>2</sub>O<sub>2</sub>, superoxide anion and hydroxyl radicals, have a key role in SCI as it can activate various pathways of apoptosis. One of the major cellular apoptosis pathways involves signaling via the death receptor CD95 (Fas/APO-1). CD95 causes apoptosis by forming a death-inducing signaling complex at the receptor, containing FADD, caspase-8/10 and the caspase-8 regulator c-FLIP.<sup>3</sup> Fas-associated phosphatase-1 (FAP-1) is an apoptosis

inhibitor that regulates the CD95-induced apoptotic signaling.<sup>4</sup> A negative correlation between FAP-1 expression and CD95-mediated cell apoptosis has been observed in various cell types.<sup>5–8</sup>

The cellular mechanisms involved in SCI are complex. MicroRNAs (miRNAs) are a class of endogenous non-coding single-stranded RNAs, which are widely involved in regulating gene expression. By binding to the 3'-untranslated region, miRNAs can suppress gene expression. Aberrant miRNA expression has also emerged as a key regulator in secondary SCI.<sup>9</sup> MiR-200c was demonstrated to be significantly upregulated following H<sub>2</sub>O<sub>2</sub> treatment.<sup>10</sup> However, little research has been conducted on the expression of miR-200c after SCI. In this regard, we explored the miRNA expression profile after SCI in mice. Furthermore, the correlation between ROS production and the altered expression of miR-200c in BV-2 cells was explored, thereby elucidating its special role in the functional recovery from SCI.

## MATERIALS AND METHODS

### Cell culture

The immortalized murine BV-2 cell line was purchased from the Chinese Academy of Medical Science and cultured in DMEM/F12 (Hyclone, Waltham, MA, USA) supplemented with 10% fetal bovine serum (Hyclone), 100 U ml<sup>-1</sup> penicillin and streptomycin in 25-cm<sup>2</sup> culture flasks at 37 °C in a humidified atmosphere with 5% CO<sub>2</sub>.

<sup>1</sup>Department of Orthopaedics, The First Affiliated Hospital, Liaoning Medical University, Jinzhou, People's Republic of China and <sup>2</sup>Department of Orthopaedics, The First Affiliated Hospital, China Medical University, Shenyang, People's Republic of China

Correspondence: Dr DS Yu, Department of Orthopaedics, The First Affiliated Hospital, Liaoning Medical University, No.2 Section 5, Renmin Road, Guta District, Jinzhou 121001, People's Republic of China.

E-mail: yudeshui8633@163.com

Received 2 July 2014; revised 29 August 2014; accepted 29 September 2014; published online 2 December 2014

## Drug treatments

Cells were treated with the following drugs. H<sub>2</sub>O<sub>2</sub> (30% w/w solution; Sigma, St Louis, MO, USA) was administered to the cells as a 100 mM solution in phosphate-buffered saline (PBS). *N*-acetyl-L-cysteine (Sigma) was dissolved in water.

## Transient transfections

Shortly before transfection,  $1.5 \times 10^5$  cells were seeded per well in a six-well plate in 2 ml DMEM culture medium containing serum and antibiotics. Before transfection, the cells were incubated under normal growth conditions (typically 37 °C and 5% CO<sub>2</sub>). Then, miR-200c mimics, miR-200c inhibitor or miR negative control (Genepharma, Shanghai, China) were pre-incubated with HiperFect transfection reagent (Qiagen, Suzhou, China) with the final concentration of miRNA analogs at 100 nmol l<sup>-1</sup>.

## RNA extraction and reverse transcription quantitative PCR

Total RNA was extracted from cell lines with Trizol (Invitrogen, Carlsbad, CA, USA) according to the manufacturer's instructions. To detect and quantify mature miR-200a, miR-200b, miR-200c, miR-141, TaqMan MicroRNA Reverse Transcription kit and TaqMan MicroRNA Assay were applied according to the manufacturer's instructions (Applied Biosystems, Foster City, CA, USA). U6 RNA was applied to be normalized. To quantify miRNA levels, 10 ng of the total RNA was reverse transcribed using TaqMan MicroRNA Reverse Transcription Kit (Applied Biosystems) with specific primers for miR-200a, miR-200b, miR-200c, miR-141 and U6. Subsequently, the PCR amplifications were performed in 20 µl reaction volumes containing 10 µg TaqMan 2 × Universal PCR Master Mix, 1 µl 20X TaqMan MicroRNA Assay mix (Applied Biosystems) and 1.33 µl template cDNA in the same system used for mRNA quantitation. The thermal cycling conditions were, a hot start step at 95 °C for 10 min, followed by 40 cycles at 95 °C for 15 s and 60 °C for 1 min. Relative miRNA expression of miR-200c was normalized against the endogenous control, U6 RNA, using the comparative  $\Delta\Delta C_T$  method. Bio-Rad CFX Manager Software (Bio-Rad, Hercules, CA, USA) was used for quantitation analysis for both mRNA and miRNA. The primers for reverse transcription quantitative PCR are as follows (5'–3'):

miR-200a; 5'-GTCGTATCCAGTGCAGGGTCCGAGGTATTCCGCACTGGA TACGACACAATCG-3', miR-200b; 5'-GTCGTATCCAGTGCAGGGTCCGAG GTATTCCGCACTGGATACGACTCATCA-3', miR-200c; 5'-GTCGTATCCA GTGCAAGGGTCCGAGGTATTCCGCACTGGATACGACTCCATC-3', miR-141; 5'-GTCGTATCCAGTGCAGGGTCCGAGGTATTCCGCACTGGATACGACCC ATCT-3', U6; 5'-GTCGTATCCAGTGCAGGGTCCGAGGTATTCCGCACTG GATACGACAAATATG-3'. The primers used for real-time PCR were as follows (5'–3'): miR-200a forward; 5'-GCTAACACTGTCTGGTAACG ATGT, miR-200b forward; 5'-GCGTAATACTGCCTGGTAATCATG-3', miR-200c forward; 5'-GTAATACTGCCGGTAATGATGGA-3', miR-141 forward; 5'-GGCCGTTAAGACTGTCTGGTAA-3', U6 forward; 5'-GCGCGT CGTGAAGCGTTC-3', universal reverse primer, 5'-GTGCAGGGTCCGA GGT-3'.

## Western blotting analyses

BV-2 cells were firstly treated with RIPA buffer (SolarBio, Beijing, China) containing 1% (v/v) PMSF (SolarBio), 0.3% (v/v) protease inhibitor (Sigma) and 0.1% (v/v) phosphorylated proteinase inhibitor (Sigma). Then, the supernatants were extracted from the lysates after they were centrifuged at 12 000 r.p.m. at 4 °C for 15 min. And the proteins with equal amounts of 15 µg was separated on an SDS-PAGE gel (10% (v/v) polyacrylamide) and transferred onto a polyvinylidene fluoride membrane at 300 mA for 2 h as previously reported.<sup>10</sup> The primary antibodies were listed as follows: GAPDH, cleaved-caspase-3, Bcl-2, Bax, Bim and FAP-1 (Cell Signaling, Danvers, MA, USA). The protein bands were quantified using a PhosphorImager and ImageQuant (Amersham Biosciences, Piscataway, NJ, USA) software analysis.

## Apoptosis assay

To detect the effects of miR-200c on BV-2 cell apoptosis, the cells (50–60% confluent) were transfected with miR-200c mimics, inhibitor or negative control. After treatment, the cells were washed with 1 × PBS for three

times. Then, an Annexin-V FITC –PI Apoptosis Kit (Invitrogen) was applied to determine the apoptotic rate by flow cytometry. This assay employs fluorescein-labeled Annexin-V in concert with propidium iodide to detect the cells undergoing apoptosis.

## Dihydroethidium staining

Cells cultured on six-well chamber slides were washed with PBS three times for 5 min per wash, and then the slides were incubated with ROS Fluorescent Probe-dihydroethidium (Vigorous Biotechnology Beijing Co., Ltd, Beijing, China) in serum-free DMEM F12 medium for 30 min at 37 °C in darkness, fixed in 4% paraformaldehyde for 30 min at room temperature (RT). The slides were washed again and mounted. Immunofluorescence images were captured by fluorescence microscopy.

## Immunofluorescence

Cells grown on chamber slides were washed with PBS for 15 min (total), fixed in 4% paraformaldehyde for 30 min at RT and permeabilized with 0.1% TritonX-100 at RT for 5 min. After three washes with PBS for 15 min (total), nonspecific binding was blocked with 3% bovine serum albumin in PBS for 1 h at RT. Next, the cells were incubated with the following primary antibodies: murine FAP-1 and GAPDH (Cell Signaling). Then, the cells were washed with PBS and incubated with TRITC-conjugated anti-mouse IgG (Zhongshan Biotechnology, Beijing, China). After several washes 15 min (total) with PBS, the cell nuclei were visualized with Hoechst 33258 staining at a concentration of 10 µg ml<sup>-1</sup> for 10 min at RT. The slides were then examined using a fluorescence microscope.

## Statistical analysis

The data were expressed as the mean ± s.e.m. The number of independent experiments was represented by 'n'. Multiple comparisons were performed using one-way analysis of variance followed by Tukey's multiple-comparison test, where  $P < 0.05$  was considered significant.

## RESULTS

### Oxidative stress modulated miR-200c expression

To profile the expression of miRNAs after SCI, miRNA microarray was applied and the result of miRNA microarray showed that miR-200c was increased the most after SCI in mice (Figure 1a). The result of miRNA microarray was verified by quantitative PCR. As shown in Figure 1b, miR-200c was increased by 6.7, 11.2 and 5.6-fold at 3, 7 and 14 days, respectively. As SCI was usually accompanied by significant ROS production in microglia cells, murine BV-2 cells were treated with 100 µM H<sub>2</sub>O<sub>2</sub> for 10 h. Dihydroethidium staining showed that H<sub>2</sub>O<sub>2</sub> significantly enhanced ROS production (Figure 1c). Furthermore, flow cytometry analysis revealed that H<sub>2</sub>O<sub>2</sub> increased ROS levels more than threefold compared with the control (Figure 1d). After murine BV-2 cells were exposed to 100 µM H<sub>2</sub>O<sub>2</sub> for 10 h, the levels of miR-200s family were determined. As shown in Figure 1e, miR-200c was upregulated after 2 h exposure of H<sub>2</sub>O<sub>2</sub> and its expression reached the peak (6.3-fold induction) at 16 h (Figure 1e). Moreover, miR-200c induction was dose dependent at H<sub>2</sub>O<sub>2</sub> concentrations of 100–400 µM (Figure 1f). In comparison, no significant induction of miR-200a and miR-200b was found with H<sub>2</sub>O<sub>2</sub> treatment. Meanwhile, miR-141 was found to be upregulated but to a much lower level (Figures 1e and f). Thus, in this paper, miR-200c was selected owing to the significant induction by ROS production in murine BV-2 cells.

### ROS production induced apoptosis in murine BV-2 cells by enhancing cleaved-caspase3 expression

Because previous studies have established that miR-200c can induce apoptosis.<sup>11</sup> Thus, we examined the effect of H<sub>2</sub>O<sub>2</sub> on apoptosis in BV-2 cells. When murine BV-2 cells were exposed to 100 µM H<sub>2</sub>O<sub>2</sub>

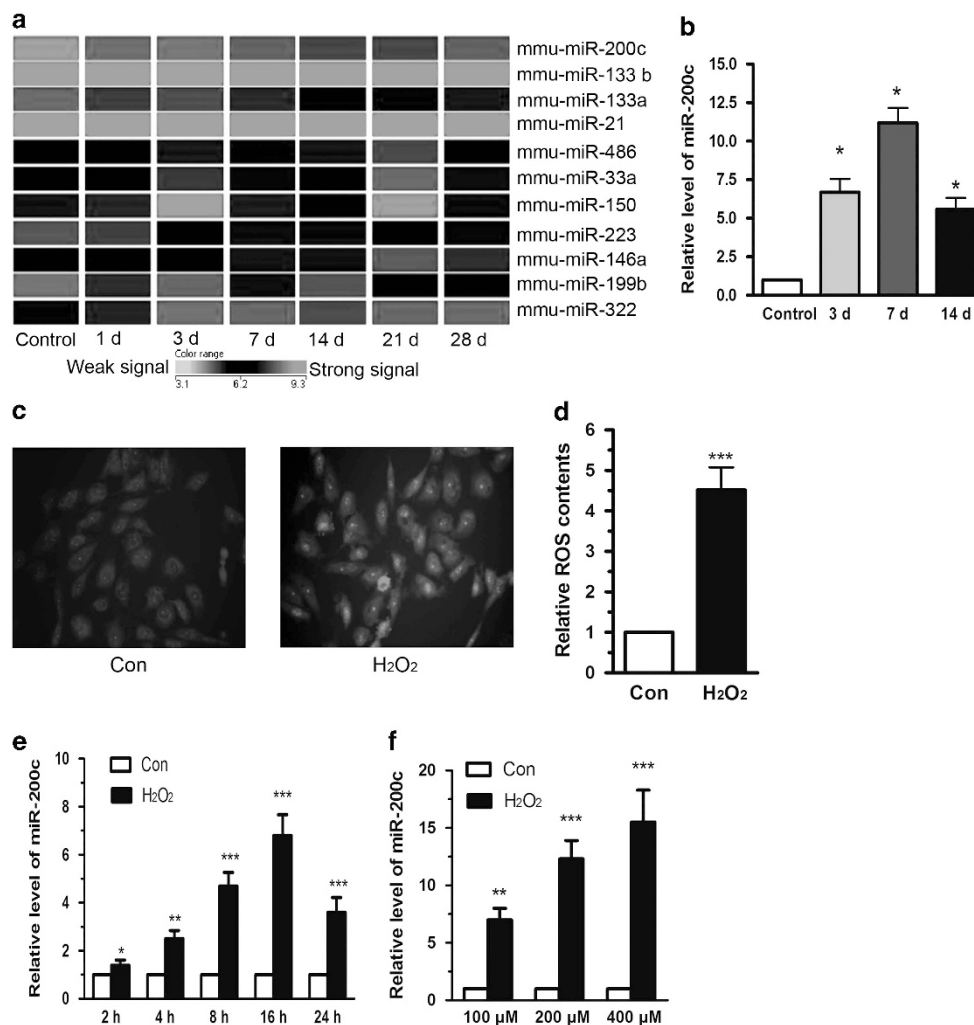


**Figure 1** Oxidative stress induced miR-200c expression in murine BV-2 cells. (a) miRNA microarray was applied to determine the changed miRNA expression profile after SCI in mice. (b) The result of miRNA microarray was verified by quantitative PCR. Murine BV-2 cells were exposed to 100 μM H<sub>2</sub>O<sub>2</sub> for 10 h. ROS production was determined using dihydroethidium staining (c) and flow cytometry. (d, e) Murine BV-2 cells were exposed to 100 μM H<sub>2</sub>O<sub>2</sub> for 2, 4, 8, 16 and 24 h; miR-200a, miR-200b, miR-200c and miR-141 levels were determined using reverse transcription quantitative PCR, at each time point. H<sub>2</sub>O<sub>2</sub> enhanced miR-200c and the peak expression was achieved after 16 h exposure to oxidative stress. (f) Murine BV-2 cells were exposed to 100, 200 or 400 μM H<sub>2</sub>O<sub>2</sub> for 16 h and relative levels of miR-200a, miR-200b, miR-200c and miR-141 were determined. miR-200c induction was dose dependent at H<sub>2</sub>O<sub>2</sub> concentrations of 100–400 μM. Data represent the means ± s.e.m., *n* = 3 independent experiments. \**P* < 0.05, \*\**P* < 0.01, \*\*\**P* < 0.001 versus control.

for 16 h, the levels of cleaved-caspase3 were significantly enhanced, as shown by western blot analysis (Figure 2a). The upregulated cleaved-caspase3 induced apoptosis through enhanced protein levels of Bax and Bim as well as reduced expression of the Bcl-2 protein. However, a pretreatment with the ROS scavenger *N*-acetylcysteine significantly reversed the H<sub>2</sub>O<sub>2</sub>-induced upregulation of cleaved-caspase3, thereby inhibiting the downstream apoptotic signaling (Figure 2a). Hoechst staining further showed obvious cellular apoptosis following H<sub>2</sub>O<sub>2</sub> exposure (Figure 2b). Notably, cell growth was also significantly reduced upon H<sub>2</sub>O<sub>2</sub> exposure, whereas scavenging ROS production with *N*-acetylcysteine reversed this effect (Figure 2c). These data indicate that ROS production induced apoptosis in murine BV-2 cells by enhancing cleaved-caspase3 expression.

#### miR-200c regulated murine BV-2 cell viability

To determine the effect of miR-200c on cell viability, murine BV-2 cells were transfected with miR-200c mimics, inhibitor or negative

control for 24, 48 and 72 h. As shown in Figure 3a, the upregulation of miR-200c by the mimics reduced cell viability by 30 and 47% at 48 and 72 h, respectively, whereas the downregulation of miR-200c by the inhibitor enhanced cell viability by 32 and 42% at 48 and 72 h, respectively (Figure 3b). These results demonstrate that miR-200c could modulate the viability of murine BV-2 cells.

#### miR-200c upregulation induced apoptosis in murine BV-2 cells

We next determined that the upregulation of miR-200c enhanced apoptosis by nearly 1.8-fold versus the negative control in murine BV-2 cells (Figure 4a). Hoechst 33342 staining also showed higher apoptosis in murine BV-2 cells transfected with miR-200c mimics compared with the negative control (Figure 4b). Altogether, these data indicate that the upregulation of miR-200c induced apoptosis in murine BV-2 cells. Furthermore, western blot analysis of apoptotic protein expression showed that the upregulation of miR-200c reduced the levels of Bcl-2 and enhanced those of Bax and Bim (Figure 4c).

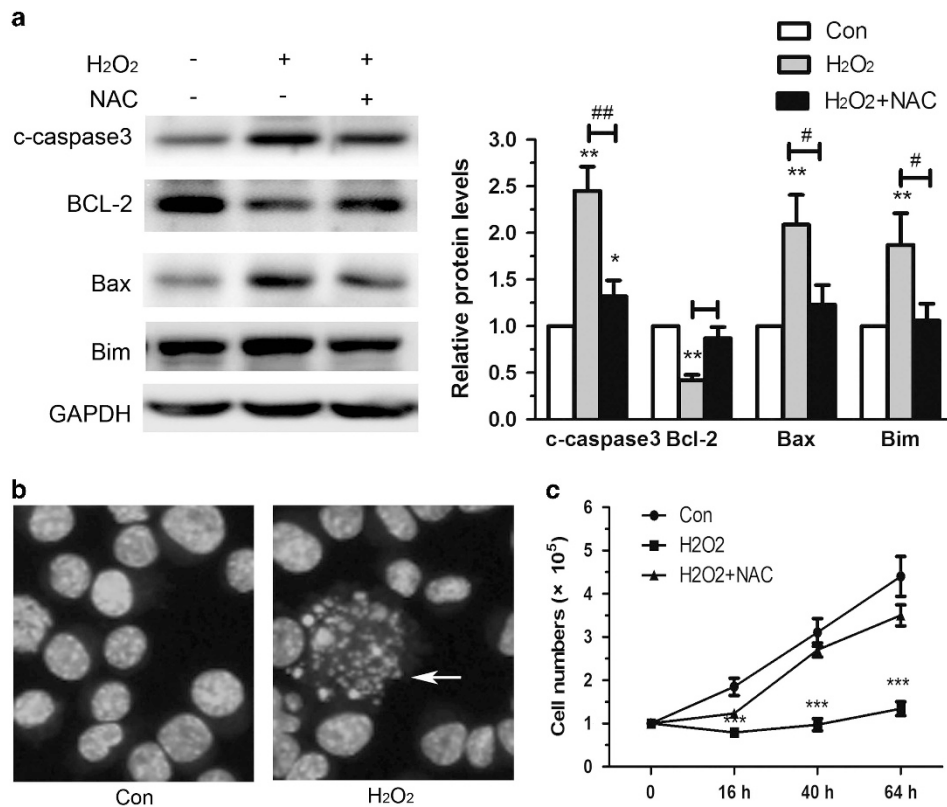


**Figure 2** ROS production induced apoptosis in murine BV-2 cells by enhancing cleaved-caspase3 expression. (a) Murine BV-2 cells were exposed to 100  $\mu$ M H<sub>2</sub>O<sub>2</sub> with or without pre-incubation with 10 mM *N*-acetylcysteine (NAC) for 16 h and FAP-1 protein was evaluated by western blotting analysis. (b) Cell apoptosis was identified using Hoechst staining with H<sub>2</sub>O<sub>2</sub> exposure. (c) Cell numbers were determined when exposed to 100  $\mu$ M H<sub>2</sub>O<sub>2</sub> with or without pre-incubation with 10 mM NAC for 16 h. Data represent the means  $\pm$  s.e.m.,  $n=3$  independent experiments. \* $P<0.05$ , \*\* $P<0.01$ , \*\*\* $P<0.001$  versus control. # $P<0.05$ , ## $P<0.01$  versus H<sub>2</sub>O<sub>2</sub>+NAC.

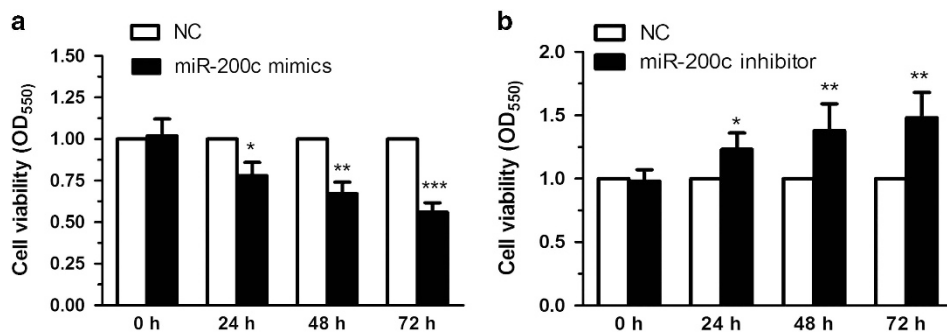


**Figure 3** MiR-200c regulated murine BV-2 cell viability. Murine BV-2 cells were transfected with miR-200c mimics, inhibitor or negative control for 24, 48 and 72 h. Upregulation of miR-200c decreased cell viability by 30 and 47% at 48 and 72 h, (a) whereas the downregulation of miR-200c enhanced cell viability in the murine BV-2 cells by 32 and 42% at 48 and 72 h, respectively (b), as analyzed by MTT assay. Data represent the means  $\pm$  s.e.m.,  $n=6$  independent experiments. \* $P<0.05$  versus control.

The suppression of miR-200c with the specific inhibitor restored the expression of Bcl-2 and reduced the levels of Bax and Bim (Figure 4d). Western blot analysis showed that the level of Bcl-2 was reduced and the levels of Bax and Bim were enhanced in BV-2 cells treated with 400  $\mu$ M H<sub>2</sub>O<sub>2</sub> for 16 h (Figure 4e). By contrast, the downregulation of miR-200c enhanced the expression of Bcl-2 and decreased Bax and Bim levels. Importantly, transfection with the miR-200c inhibitor blocked the effects of H<sub>2</sub>O<sub>2</sub> treatment on the expression of Bcl-2, Bax and Bim (Figure 4e). Taken together, these results indicate that

miR-200c may induce apoptosis in murine BV-2 cells partially through the regulation of Bcl-2, Bax and Bim expression.

#### FAP-1 was the target gene of miR-200c

Because a previous report identified FAP-1 as the target gene of miR-200c, we tested the impact of miR-200c on FAP-1 expression.<sup>11</sup> As shown in Figure 5a, when murine BV-2 cells were transfected with miR-200c mimics, FAP-1 protein levels were significantly reduced, along with the activation of cleaved-caspase3. By contrast, transfection



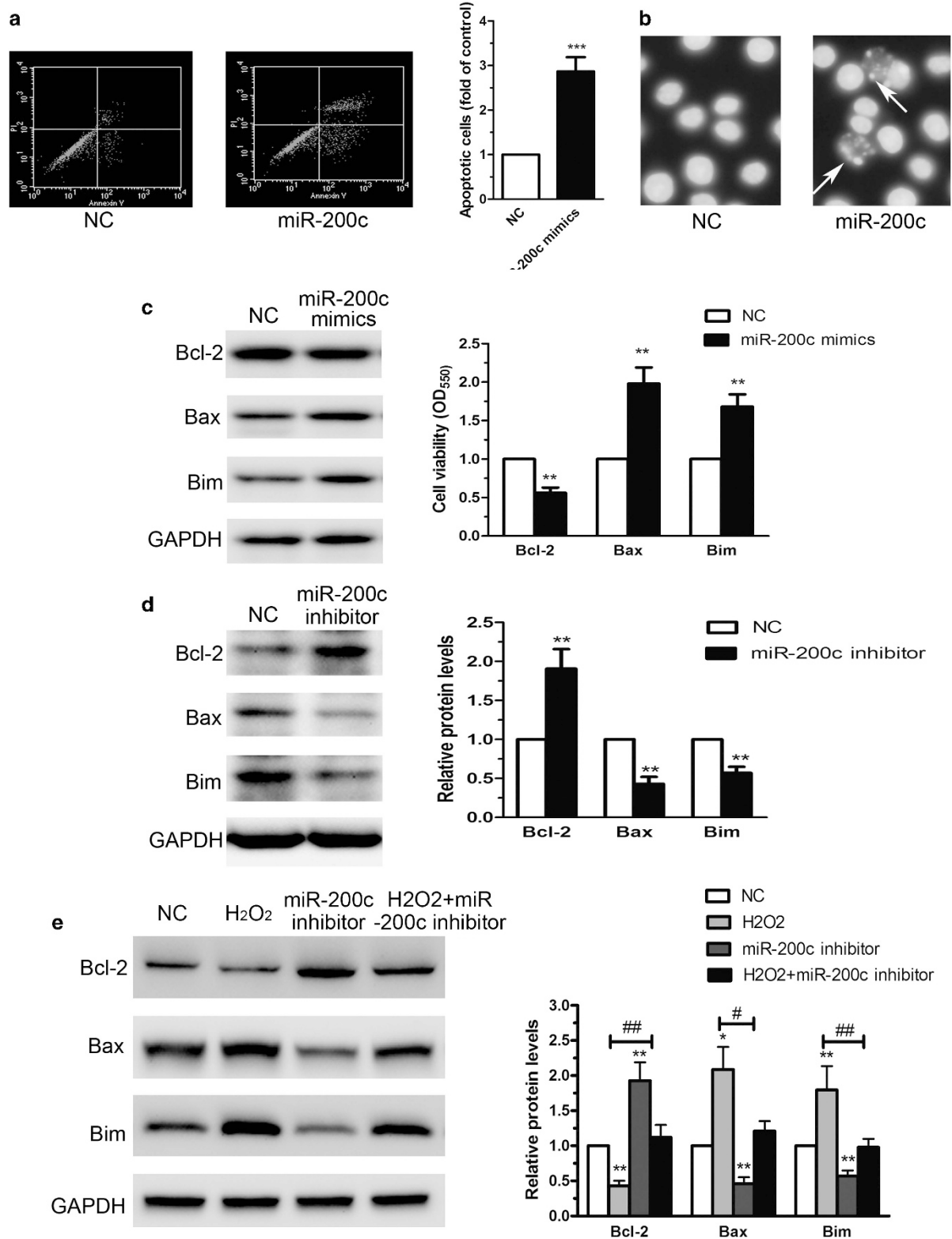


**Figure 4** Upregulation of miR-200c induced murine BV-2 cell apoptosis. MiR-200c mimics or inhibitor were transfected into murine BV-2 cells for 48 h. Upregulation of miR-200c enhanced cell apoptosis by 1.8-fold versus negative control in murine BV-2 cells, (a) as tested by Annexin-V and propidium iodide kit. (b) The apoptotic cells increased in the murine BV-2 cells transfected with miR-200c mimics, as examined by Hoechst 33342 staining. White arrow indicated apoptotic cells. As assessed by western blot, upregulation of miR-200c could decrease the level of Bcl-2 and increase the levels of Bax and Bim (c), whereas suppression of miR-200c could elevate the expression level of Bcl-2, and reduced the levels of Bax and Bim (d). Transfection with the miR-200c inhibitor blocked the effects of H<sub>2</sub>O<sub>2</sub> treatment on the expression of Bcl-2, Bax and Bim (e). Data represent the means  $\pm$  s.e.m.,  $n=3$  independent experiments. \* $P<0.05$  versus control; \*\* $P<0.01$  versus control; # $P<0.05$  versus H<sub>2</sub>O<sub>2</sub> + miR-200c inhibitor; ## $P<0.01$  versus H<sub>2</sub>O<sub>2</sub> + miR-200c inhibitor.

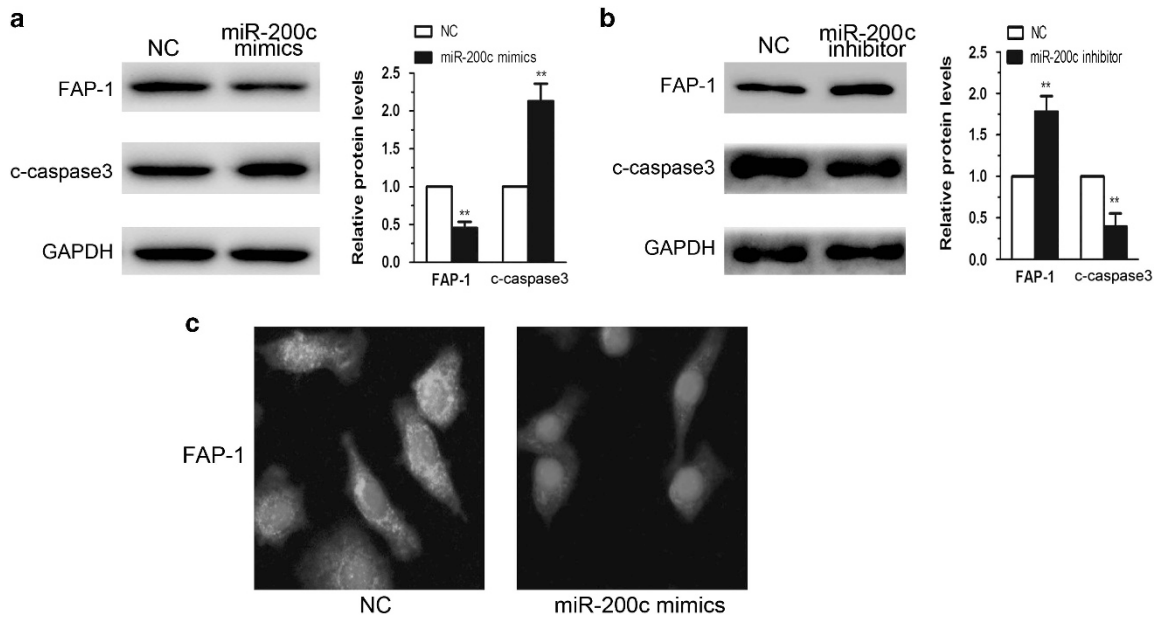


**Figure 5** FAP-1 was the host gene of miR-200c. As analyzed by Western blot, overexpression of miR-200c reduced the protein level of FAP-1 and activated cleaved-caspase3 (a), while suppression of miR-200c enhanced FAP-1 level and reduced cleaved-caspase3 (b). (c) Immunofluorescence revealed that FAP-1 was significantly reduced in the murine BV-2 cells transfected with miR-200c mimics for 48 h. Data represent the means  $\pm$  s.e.m.,  $n=3$  independent experiments. \* $P<0.05$ , \*\* $P<0.01$  versus control.

with the miR-200c inhibitor enhanced FAP-1 expression and reduced cleaved-caspase3 levels (Figure 5b). To further confirm that FAP-1 is negatively regulated by miR-200c, FAP-1 expression was analyzed by immunofluorescence. We found that FAP-1 levels were significantly reduced after transfection with miR-200c mimics, compared with the negative control (Figure 5c). These data indicate that miR-200c negatively regulated the expression of FAP-1, thereby inducing FAS signaling-induced apoptosis.

#### FAP-1 downregulation was required for miR-200c-mediated apoptosis in murine BV-2 cells

We next investigated whether the downregulation of FAP-1 is an integral part of miR-200c-induced apoptosis. To this end, miR-200c was inhibited in murine BV-2 cells in the presence of a small interfering RNA (siRNA) targeting FAP-1. As shown in Figure 6a, the silencing of FAP-1 significantly enhanced cleaved-caspase3 activation, thus triggering downstream effects, such as enhanced Bax expression and reduced Bcl-2 expression. More importantly, miR-200c inhibition failed to reduce cleaved-caspase3 expression in murine BV-2 cells that were transfected with siRNA-FAP-1 (Figure 6a). Reverse transcription quantitative PCR analysis showed that the FAP-1-targeting siRNA did not affect the level of miR-200c in murine BV-2 cells. In addition, transfection of the miR-200c inhibitor alone led to reduced apoptosis, whereas suppression of FAP-1 by siRNA promoted apoptosis, even in cells that were co-transfected with the miR-200c inhibitor (Figure 6c). Taken together, these results indicate that miR-200c promoted apoptosis in murine BV-2 cells by reducing FAP-1 expression.

#### DISCUSSION

After SCI, multiple molecular and biochemical changes occur, including aberrations in mRNA levels, protein expression, inflammatory factor secretion, ROS production and neural cell apoptosis and death.<sup>12</sup> Many studies have addressed the altered mRNA and protein

levels after SCI as well as their correlation with SCI pathophysiology. MicroRNAs are a class of small non-coding single-stranded RNA molecules. miRNAs are known to repress gene expression by binding to the 3'-untranslated region (3'-UTR). An abnormal miRNA expression profile following SCI was suggested to affect SCI pathophysiology and functional recovery.<sup>13</sup> For instance, miR-21 was significantly upregulated 3 days after SCI in rats and showed strong anti-apoptotic effects, thus indicating its protective role after SCI.

Growing evidence supports the key role of ROS production in cellular apoptosis after SCI, yet the specific mechanisms remain unclear.<sup>14</sup> In this study, we treated murine BV-2 cells with H<sub>2</sub>O<sub>2</sub> to generate a cellular model of SCI. By using reverse transcription quantitative PCR analysis, we found the expression pattern of some miRNAs to be significantly altered. According to our data, miR-200c upregulation started 2 h after H<sub>2</sub>O<sub>2</sub> treatment and achieved its peak at 16 h. miR-200c expression was enhanced by the H<sub>2</sub>O<sub>2</sub> treatment in a dose-dependent manner. Oxidative stress has a key role in various pathologies; many studies have explored an underlying mechanism, by which ROS production regulates cellular apoptosis.<sup>15</sup> Here, we have explored the effect of ROS production on apoptosis in murine BV-2 cells. As shown in Figure 2, ROS production in BV-2 cells significantly induced caspase-3-activated apoptosis and inhibited cell growth. Thus far, little research has addressed ROS-induced miRNA alterations in murine BV-2 cells and their effects on spinal cord functional recovery.<sup>13</sup>

MiR-200c belongs to the miR-200 family that has been reported to regulate the epithelial-to-mesenchymal transition in various cancer cells and tissues.<sup>16-18</sup> In tumors, miR-200 expression is significantly reduced, which promotes the epithelial-to-mesenchymal transition and thus enhances cancer cell aggressiveness and metastasis. By contrast, the introduction of miR-200 inhibits cancer cell growth. In line with these observations, we found that the ROS-induced upregulation of miR-200c significantly inhibited cell growth, whereas the inhibition of miR-200c increased cell viability. These findings

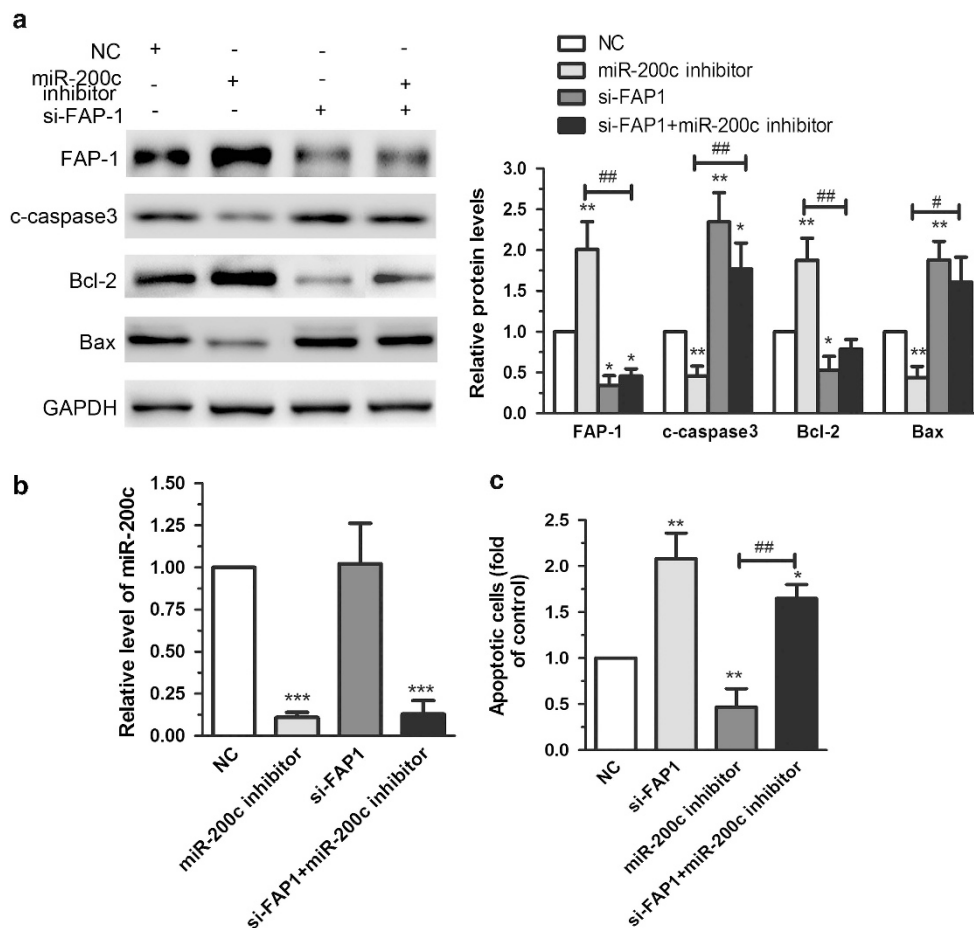


**Figure 6** MiR-200c induced cell apoptosis by reducing FAP-1 expression. Downregulation of miR-200c elevated the expression of FAP-1 and reduced cleaved-caspase3 protein level, whereas silencing of FAP-1 reduced Bcl-2 expression. More significantly, downregulation of miR-200c could no longer decrease the level of cleaved-caspase3 in the murine BV-2 cells transfected with siRNA-FAP-1 (a) Downregulation of FAP-1 did not affect the level of miR-200c in the murine BV-2 cells, as shown by reverse transcription quantitative PCR. (b) Downregulation of FAP-1 by siRNA promoted apoptosis, even in cells that were co-transfected with the miR-200c inhibitor. (c) Data represent the means  $\pm$  s.e.m.,  $n=3$  independent experiments. \* $P<0.05$  versus control; \*\* $P<0.01$  versus control; \*\*\* $P<0.001$  versus control. ## $P<0.01$  versus si-FAP-1+miR-200c inhibitors.

indicate that miR-200c upregulation may contribute to ROS-induced apoptosis in BV-2 cells after SCI.

miR-200c upregulation in murine BV-2 cells was found to induce apoptosis through enhanced Bax and Bim expression and reduced Bcl-2 protein levels. Notably, similar effects were observed upon  $H_2O_2$  treatment. Conversely, the inhibition of miR-200c significantly promoted cell growth, with decreased protein levels of Bax and Bim and enhanced Bcl-2 expression (Figure 4); similar effects were induced by the ROS scavenger (*N*-acetylcysteine). To address the specific mechanism by which miR-200c induced apoptosis, we tested the impact of miR-200c on FAP-1, which had been shown to be repressed by miR-200c in several cancer cells.<sup>11</sup> FAP-1 is known to be a negative regulator of CD95-induced apoptosis.<sup>19,20</sup> Western blot analysis revealed that the overexpression of miR-200c reduced FAP-1 protein levels, whereas the subsequent inhibition of miR-200c enhanced FAP-1 expression, thereby demonstrating enhanced anti-apoptotic effects. These results indicate that miR-200c induced apoptosis in BV-2 cells mainly by suppressing FAP-1 expression.

Significantly, silencing the FAP-1 expression with a specific siRNA caused the same pro-apoptotic effects as miR-200c upregulation, thus correlating FAP-1 reduction with miR-200c upregulation. Furthermore, in BV-2 cells that were transfected with a FAP-1-targeting

siRNA, even transfection with miR-200c inhibitors would not reverse FAP-1 inhibition-induced cell apoptosis. These results indicate that the miR-200c overexpression-induced apoptosis in BV-2 cells was mainly achieved by inhibition of FAP-1.

In summary, this study demonstrates that miR-200c is upregulated by ROS production in murine BV-2 cells and that the overexpression of miR-200c induces significant apoptosis. We have shown FAP-1, which inhibits CD95-mediated cell apoptosis, to be a direct target of miR-200c. Our finding indicates that the upregulation of miR-200c expression enhances apoptosis and inhibits functional recovery in the BV-2 cell model, which may represent a therapeutic target for enhancing neural cell functional recovery after SCI.

#### DATA ARCHIVING

There were no data to deposit.

#### CONFLICT OF INTEREST

The authors declare no conflict of interest.

#### ACKNOWLEDGEMENTS

This work was supported by Doctoral Scientific Research Starting Foundation of Liaoning Province, No. 20121096; Program for Liaoning Excellent Talents in

University, No. LR2013091; Scientific Research Starting Foundation for PH.D. and Returned Overseas Teacher of Liaoning Medical University, No. Y2012B011; Special Funds for Clinical Medicine Construction of the Principal's Fund of the Liaoning Medical University, No. XZJJ20130241; National Natural Science Foundation of China, Nos 81171799, 81272074 and 81471853.

- 1 Vidal PM, Lemmens E, Avila A, Vanganswinkel T, Chalaris A, Rose-John S *et al*. ADAM17 is a survival factor for microglial cells *in vitro* and *in vivo* after spinal cord injury in mice. *Cell Death Dis* 2013; **12**: e954.
- 2 Chatterjee D, Biswas K, Nag S, Ramachandra SG, Das Sarma J. Microglia play a major role in direct viral-induced demyelination. *Clin Dev Immunol* 2013; **2013**: 510396.
- 3 Peter ME, Krammer PH. The CD95(APO-1/Fas) DISC and beyond. *Cell Death Differ* 2003; **10**: 26–35.
- 4 Miyazaki T, Atarashi Y. Fas-associated phosphatase-1 promotes Fas-mediated apoptosis in human colon cancer cells: novel function of FAP-1. *J Gastroenterol Hepatol* 2006; **2**: 84–91.
- 5 Elnemr A, Ohta T, Yachie A, Kayahara M, Kitagawa H, Fujimura T *et al*. Human pancreatic cancer cells disable function of Fas receptors at several levels in Fas signal transduction pathway. *Int J Oncol* 2001; **18**: 311–316.
- 6 Foehr ED, Lorente G, Vincent V, Nikolich K, Urfer R. FAS associated phosphatase (FAP-1) blocks apoptosis of astrocytomas through dephosphorylation of FAS. *J Neurooncol* 2005; **74**: 241–248.
- 7 Ivanov VN, Lopez Bergami P, Maulit G, Sato TA, Sassoon D, Ronai Z. FAP-1 association with Fas (Apo-1) inhibits Fas expression on the cell surface. *Mol Cell Biol* 2003; **23**: 3623–3635.
- 8 Meinhold-Heerlein I, Stenner-Liewen F, Liewen H, Kitada S, Krajewska M, Krajewski S *et al*. Expression and potential role of Fas-associated phosphatase-1 in ovarian cancer. *Am J Pathol* 2001; **158**: 1335–1344.
- 9 Kosik KS. The neuronal microRNA system. *Nat Rev Neurosci* 2006; **7**: 911–920.
- 10 Magenta A, Cencioni C, Fasanaro P, Zaccagnini G, Greco S, Sarra-Ferraris G *et al*. miR-200c is upregulated by oxidative stress and induces endothelial cell apoptosis and senescence via ZEB1inhibition. *Cell Death Differ* 2011; **18**: 1628–1639.
- 11 Schickel R, Park SM, Murmann AE, Peter ME. miR-200c regulates induction of apoptosis through CD95 by targeting FAP-1. *Mol Cell* 2010; **38**: 908–915.
- 12 Di Giovanni S, Knobloch SM, Brandoli C, Aden SA, Hoffman EP, Faden AI. Gene profiling in spinal cord injury shows role of cell cycle in neuronal death. *Ann Neurol* 2003; **53**: 454–468.
- 13 Hu JZ, Huang JH, Zeng L, Wang G, Cao M, Lu HB. Anti-apoptotic effect of microRNA-21 after contusion spinal cord injury in rats. *J Neurotrauma* 2013; **30**: 1349–1360.
- 14 Kim D, You B, Jo EK, Han SK, Simon MI, Lee SJ. NADPH oxidase 2-derived reactive oxygen species in spinal cord microglia contribute to peripheral nerve injury-induced neuropathic pain. *Proc Natl Acad Sci USA* 2010; **107**: 14851–14856.
- 15 Chen S, Ren Q, Zhang J, Ye Y, Zhang Z, Xu Y *et al*. N-acetyl-L-cysteine protects against cadmium-induced neuronal apoptosis by inhibiting ROS-dependent activation of Akt/mTOR pathway in mouse brain. *Neuropathol Appl Neurobiol* 2013; **40**: 759–777.
- 16 Wellner U, Schubert J, Burk UC, Schmalhofer O, Zhu F, Sonntag A *et al*. The EMT-activator ZEB1 promotes tumorigenicity by repressing stemness-inhibiting microRNAs. *Nat Cell Biol* 2009; **11**: 1487–1495.
- 17 Liu YN, Yin JJ, Abou-Kheir W, Hynes PG, Casey OM, Fang L *et al*. MiR-1 and miR-200 inhibit EMT via Slug-dependent and tumorigenesis via Slug-independent mechanisms. *Oncogene* 2013; **32**: 296–306.
- 18 Tellez CS, Juri DE, Do K, Bernauer AM, Thomas CL, Damiani LA *et al*. EMT and stem cell-like properties associated with miR-205 and miR-200 epigenetic silencing are early manifestations during carcinogen-induced transformation of human lung epithelial cells. *Cancer Res* 2011; **71**: 3087–3097.
- 19 Wieckowski E, Atarashi Y, Stanson J, Sato TA, Whiteside TL. FAP-1-mediated activation of NF-kappaB induces resistance of head and neck cancer to Fas-induced apoptosis. *J Cell Biochem* 2007; **100**: 16–28.
- 20 Nakka VP, Gusain A, Mehta SL, Raghurir R. Molecular mechanisms of apoptosis in cerebral ischemia: multiple neuroprotective opportunities. *Mol Neurobiol* 2008; **37**: 7–38.